Environ. Sci. Technol. **2011,** *45,* 706–711

Conversion of Elemental Mercury with a Novel Membrane Delivery Catalytic Oxidation System (MDCOs)

YONGFU GUO,[†] NAIQIANG YAN,[*,†]
SHIJIAN YANG,[†] ZAN QU,[†]
ZHONGBIAO WU,[*,‡] YUE LIU,[‡]
PING LIU,[†] AND JINPING JIA[†]
School of Environmental Science and Engineering, Shanghai Jiao Tong University, Shanghai, 200240, China; Department of Environmental Engineering, Zhejiang University, Hangzhou 310027, China

Received June 17, 2010. Revised manuscript received November 24, 2010. Accepted November 29, 2010.

In order to overcome the shortcomings of the traditional catalytic oxidation (TCO) mode for the conversion of the trace level of elemental mercury (Hg^0) in flue gas, we put forward a novel and unique assembly that integrated membrane delivery with catalytic oxidation systems (MDCOs), which combined the controlled delivery of oxidants with the catalytic oxidation of Hg^0. The results show that the demanded HCl for Hg^0 conversion in the MDCOs was less than 5% of that in the TCO mode, and over 90% of Hg^0 removal efficiency can be obtained in the MDCOs with less than 0.5 mg m^{-3} of HCl escaped. Meanwhile, the inhibition of SO_2 to Hg^0 catalytic conversion in the MDCOs was also less significant than in the TCO. The MDCOs have high retainability for HCl, which is quite favorable to Hg^0 conversion and HCl utilization. The reaction mechanism on mercury conversion in the MDCOs is discussed. The MDCOs appear to be a promising method for emission control of elemental mercury.

Introduction

Coal-fired utilities have been considered as the largest sources of anthropogenic mercury emissions in the world (*1*). Mercury in coal-fired flue gas generally presents in gaseous elemental mercury (Hg^0), gaseous oxidized mercury (Hg^{2+}), and particulate-bound mercury (Hg^p), among which Hg^0 will be the dominant form in flue gases from low-rank coal or low-chlorine coal (*2, 3*). Hg^{2+} and Hg^p are easily to be removed from flue gas with the existing air pollution control devices (APCDs), which include particulate collectors and flue gas desulphurization devices (FGD). However, Hg^0 has been found to be the most difficult to be captured by the existing APCDs (*4, 5*). Moreover, Hg^0 emitted with flue gas is observed to be the most persistent in the atmosphere with a lifetime of up to 1 year (*2*), which will inevitably cause the long-distance transport among the countries or even continents.

One of the effective methods for Hg^0 removal is to convert Hg^0 to its oxidized form Hg^{2+}, which can be readily captured by a wet flue gas desulphurization system (WFGD) downstream. Catalytic oxidation of Hg^0 in the presence of gaseous HCl has been given much attention because HCl usually presents in flue gases (*6*). The roles of the selective catalytic reduction (SCR) of NO_x catalysts on Hg^0 catalytic oxidation have been previously investigated (*7, 8*). Although some SCR catalysts have been observed to be able to promote the oxidation of Hg^0, the conversion efficiencies are relatively low and rather high HCl is demanded to obtain higher Hg^0 conversion (*9, 10*). In addition to SCR catalysts, noble metals or some transition metal oxides have been investigated as potential mercury oxidation catalysts (*10, 11*). Among the metal oxides, manganese oxide (MnO_x) displays significant adsorption/catalysis performance on Hg^0 capture, especially in the presence of HCl. However, the demanded HCl is still high according to the previous studies, and the presence of SO_2 in flue gas also significantly inhibits Hg^0 conversion on the surface of catalysts (*11*).

In fact, among the present research on the catalytic oxidation of Hg^0 with HCl, almost all tests have been performed with the traditional catalytic oxidation (TCO) mode (Figure 1a), in which HCl is premixed with flue gas containing Hg^0 before its flow across the catalysts. According to our preliminary analysis, the TCO mode might not be an optimal way for Hg^0 conversion due to the following aspects. First, HCl is just the precursor of oxidants, which must be activated adequately through series of reactions including Deacon reaction, before it is involved in Hg^0 oxidation (*4*). Second, the concentration of Hg^0 in flue gas is only in the trace level but with high Hg^0 oxidation efficiency demanded in practice (e.g., 90%). In addition, SO_2 as an acidic component in flue gas will inevitably compete with HCl to adsorb on the surface of catalysts, which will inhibit the reactions such as Deacon reaction and Hg^0 oxidation (*8, 9*). These aspects might be the main reasons causing the low utilization efficiency of HCl for the most tested TCO mode, and all of the unreacted HCl will escape with the flue gas.

On the basis of the above consideration, a novel technology that integrated the membrane delivery of oxidants with catalytic oxidation system (MDCOs) was put forward for Hg^0 conversion, which employed a porous ceramic tube as the medium for oxidant delivery and catalyst carrier. The performance of catalytic oxidation in the MDCOs with manganese oxide as catalysts was investigated at various conditions.

Experimental Section

The Conception of the MDCOs. The conception of the MDCOs is illustrated in Figure 1b, which is compared with the TCO mode (Figure 1a). A porous tubular ceramic membrane is the main body of MDCOs, which also serves as the catalyst carrier on its outside surface. The porous wall of the membrane is used for the delivery of oxidants or precursor (e.g., HCl) by penetration from the inner chamber outward to catalyst layer with its microporous diffusion and adsorption−desorption sequences. The outside catalytic layer is directly exposed to the simulated flue gas. The mass transfer and concentration distribution of oxidants for the MDCOs and TCO are also illustrated in Figure 1 (not quantitively). As shown in Figure 1b, the oxidant (with concentration of $[X]_0$) in the inner chamber of ceramic membrane slowly releases through the porous wall and finally reaches the outside surface of the catalytic layer. During the process of delivery, HCl might be gradually activated by MnO_x catalysts. Subsequently, the activated oxidants can react with Hg^0 on the surface of the catalyst more effectively. Therefore, the

---

[*] Address correspondence to either author. Phone: +86 21 54745591 (N.Y.); +86 571 87952459 (Z.W.). Fax: +86 21 54745591 (N.Y.); +86 571 87952459 (Z.W.) e-mail: nqyan@sjtu.edu.cn (N.Y.); zbwu@zju.edu.cn (Z.W.).

[†] School of Environmental Science and Engineering, Shanghai Jiao Tong University.

[‡] Department of Environmental Engineering, Zhejiang University.

10.1021/es1020586

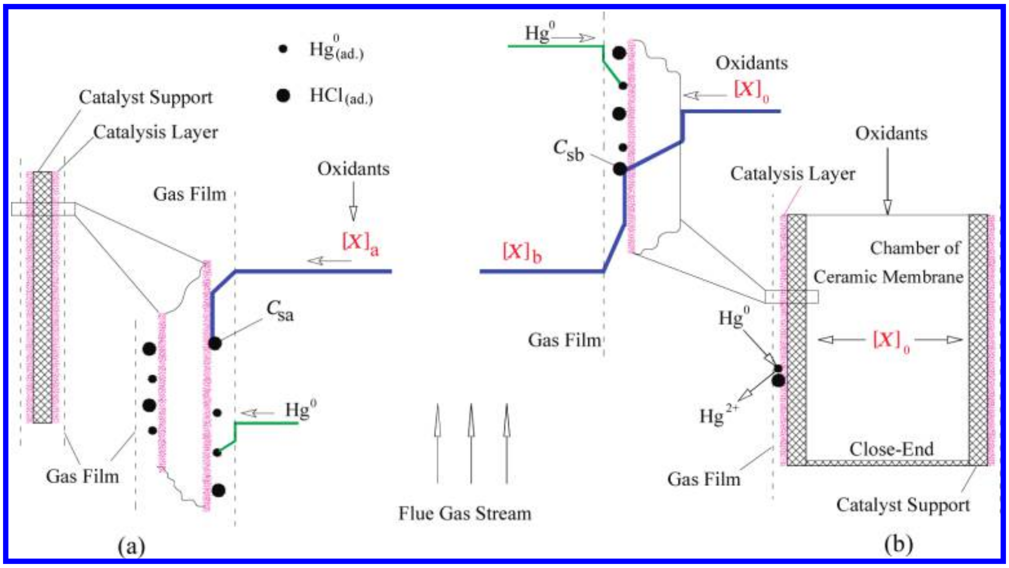

FIGURE 1. The comparison of the delivery and concentration distribution of the oxidant: (a) the TCO mode and (b) the MDCOs mode: The TCO mode meant the traditional catalytic oxidation mode, and the MDCOs mode referred to the membrane delivery catalytic oxidation mode; $[X]_a$ and $[X]_b$ denoted the employed oxidant concentration in flue gas in the TCO mode and penetrated oxidant concentration in the MDCOs, respectively. C_{sa} and C_{sb} were adsorbed oxidant concentration on the surface of catalytic layer, respectively.

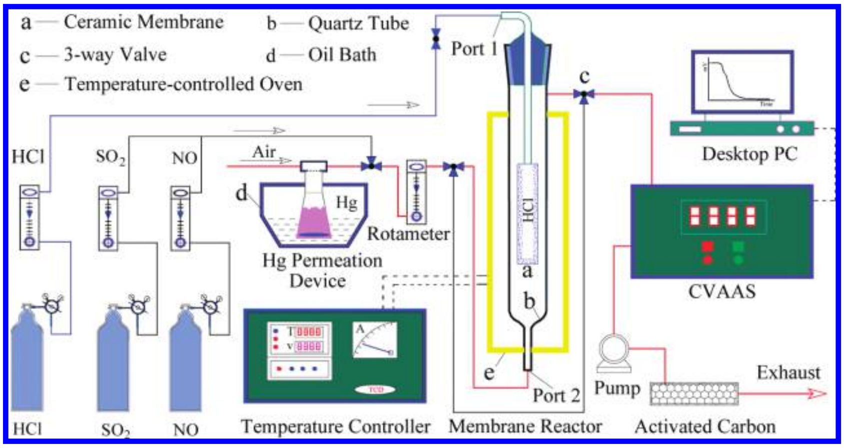

FIGURE 2. The schematic diagram of the experimental setup.

membrane serves as the delivery medium of the oxidants besides the catalyst carrier, and it may also work as the buffer medium for oxidants if the membrane material has retention capacity for oxidants or HCl.

Experimental Setup. The experimental setup shown in Figure 2 was employed to evaluate the performance of mercury catalytic oxidation in the MDCOs with MnO_x catalyst. The assembly consisted of a self-made mercury permeation device (*12*), a MDCOs reactor, an online cold vapor atomic adsorption spectrophotometry (CVAAS), and the gas preparation system.

The MDCOs reactor employed a quartz tube (360 mm in length with an inner diameter of 16 mm) as the shell, in which a tubular ceramic membrane mounted coaxially. As shown in Figure 2, injecting HCl from port 1, which was directly connected to the inner chamber of ceramic membrane, was considered as the MDCOs mode. In addition, the process can be considered as the TCO mode if HCl was injected from port 2, where HCl would be premixed with the simulated flue gas before its exposure to the catalysts. The latter was used as the reference in this work.

The CVAAS (SG-921, Jiangfen Ltd.), was used to continuously monitor and acquire the inlet (C_0) and outlet (C) Hg^0 concentration of the reactor. Besides the mercury vapor, others gases including compressed air, N_2 (as the balance gas), HCl (0−32.6 mg m^{-3}), NO (100−300 mg m^{-3}), and SO_2 (0−4000 mg m^{-3}), were all purchased from Dalian Special Gas Co. The CVAAS for mercury measurement was calibrated in the presence of various components.

Preparation of Catalysts. The MDCOs employed a porous tubular membrane made of alumina (Al_2O_3, Hefei Great Wall Co. Ltd.), with the average pore diameter of 4.7 μm (see Figure S1 in the Supporting Information (SI)), inner diameter of 8.0 mm, the outer diameter of 12.0 mm, Brunauer−Emmett−Teller (BET) surface of the membrane material of 1.42 m^2 g^{-1}, and the length of 50 mm. One end of the membrane was connected with port 1, and the other end was sealed. Catalysts of MnO_x/Al_2O_3 were prepared by the wet impregnation method and the aqueous solution of manganese nitrate (Sinopharm Chemical Reagent Co.) is the precursor. MnO_x loading value (ε) of MnO_x/Al_2O_3 is defined as follows:

$$\varepsilon = \frac{W_{Mn}}{W_{Al}} \times 100\% \qquad (1)$$

where W_{Mn} is the quantity of manganese (g) and W_{Al} is the quality of support of Al_2O_3 (g).

Analytical Methods. The X-ray diffractometer (D/max-2200/PC, Rigaku Co., Japan) was used to determine the crystal structures of the sorbents operating at 40 kV and 20 mA using

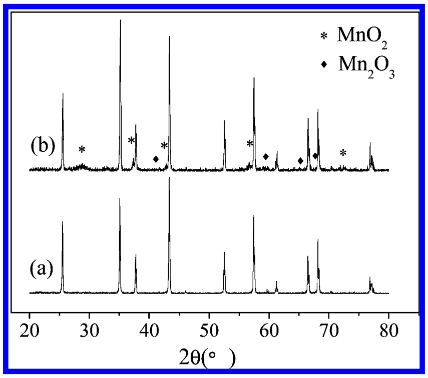

FIGURE 3. X-ray diffraction patterns: (a), virgin ceramic tube, $\varepsilon = 0$ wt.%, (b), MnO_x/Al_2O_3, $\varepsilon = 8.0$ wt.%.

Cu Kα radiation in the range of 20−80° (2θ) with a step size of 0.02°. The BET was measured using a nitrogen adsorption apparatus (Micromeritics ASAP 2010, USA). All of the samples were degassed at 453 K prior to BET measurements. The XPS analyzer (PHI-5000C ESCA) used Mg Kα radiation ($h\nu = 1253.6$ eV) as X-ray excitation source to determine the Mn 2p, Hg 4f, and O 1s binding energies. Loading value ε was quantified by the flame atomic absorption spectrometry (AAS, KLAS-1000CA, Kwicklink Chemical Co., Ltd., U.K.).

The Ontario Hydro Method (OHM) was used to test the balance of mercury before and after the conversion (*8, 12*). The measurement for HCl, Cl_2, and SO_2 was carried out with the recommended method with specific gas detector tubes (Gastec, Japan).

Results and Discussion

Characterization of Catalysts. The XRD patterns (Figure 3) indicated that the diffraction pattern of the ceramic tube was almost identical with that of α-Al_2O_3 (JCPDS 46−1212), and the primary diffraction peaks of manganese oxides were consistent with those of MnO_2 at $2\theta = 28.84°$, 37.54°, 43.34°, 56.78°, and 72.7° (JCPDS 24−0735), respectively. It was obvious that MnO_x mainly presented in the form of MnO_2 though the weak peak for Mn_2O_3 can be observed as well.

In addition, both the pore size (Figure S2 in the SI) and the BET surface area (S_{BET}) of the materials were tested. The results show that both pore size and S_{BET} became smaller with the increase of ε value. Most pores distribute at the diameter ranging from 1 to 5 μm after loaded manganese. The S_{BET} and average pore size were 0.83 $m^2\,g^{-1}$ and 1.90 μm, respectively. The total porosity decreased from 24.85% to 12.09%. In addition, MnO_x was observed to be evenly distributed across the porous wall of the membrane (Figure S3 in the SI).

Retainability and Conversion of HCl in the MDCOs. The penetration curves of HCl in the MDCOs with various ε values were investigated, and the results are shown in Figure 4. As can be seen, the ceramic membrane with MnO_x displayed significant retainability for HCl, and its capacity went up with the increase of ε value. The complete breakthrough time prolonged with the increase of ε value. The breakthrough time of HCl in the tubular membrane with ε of 0 wt.% and 8 wt.% were 3 and 26 h, respectively. And the adsorbed equilibrium amount of HCl on the membrane with ε of 8 wt.% was 0.14 mg-HCl/g-tube with 30 mg m^{-3} of HCl in the gas at 573 K. Part of HCl would desorb from the tube as the tube was swept with air without HCl. Almost all HCl desorbed reversibly from the virgin tube ($\varepsilon = 0$) according to the mass balance evaluation. However, most HCl retained in the tube wall with MnO_x cannot be desorbed reversibly, which indicated that most HCl might be chemically adsorbed on the catalyst. Therefore, the high retainability of HCl in the MDCOs would be helpful to the sequential reactions for Hg^0 oxidation.

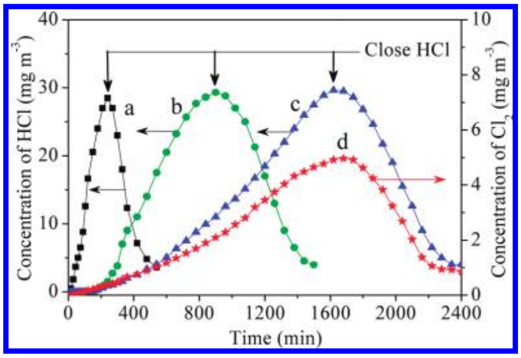

FIGURE 4. The penetration curves of HCl and Cl_2 produced in the MDCOs at 573 K without Hg^0 in the gas: Initial HCl concentration was about 30 mg m^{-3} with flow rate of 2.0 L h^{-1}; HCl injection at port 1 without the dilution gas outside the membrane. (a), HCl, $\varepsilon = 0$; (b), HCl, $\varepsilon = 2$ wt.%; (c), HCl, $\varepsilon = 8$ wt.%; and (d), the concentration of produced Cl_2, $\varepsilon = 8$ wt.%.

Previous studies have indicated that Deacon reaction might be the predominant pathway for Hg^0 oxidation by HCl in the presence of catalysts, and chlorine (Cl_2) and/or Cl atom (hydrogen abstracted from HCl) are the active intermediates (*4, 13, 14*). Therefore, Cl_2 production can be used as an identifier to evaluate the efficacy of Deacon reaction in the MDCOs. Generally, Cl_2(g) in flue gas mainly comes from the overall Deacon reaction as follows.

$$4HCl(g) + O_2(g) \xrightarrow{MnO_2} 2Cl_2(g) + 2\,H_2O(g) \qquad (2)$$

The production of Cl_2(g) in the MDCOs was monitored accompanied with HCl penetration across the membrane. Though Cl_2 was hardly detectable in the TCO mode, a higher Cl_2 yield was observed in the MDCOs and the maximum Cl_2 concentration was about 4.9 mg m^{-3} (curve d in Figure 4). The results indicate that the conversion of HCl to Cl_2 by Deacon reaction was rather effective in the MDCOs, which can be tentatively explained from the following two aspects. First, the adsorbed HCl concentration on the surface of the catalysts in the MDCOs was supposed to be higher by far than that of the TCO mode (Figure 1; Figure S4 in the SI), and the rate of Cl_2 production from Deacon reaction accordingly became rapid. Second, HCl can be adequately exposed to the catalyst as it was delivered across the porous wall of the membrane, and the Deacon reaction can occur simultaneously.

Catalytic Oxidation of Hg^0 in the MDCOs. To further investigate the delivery performance of HCl on Hg^0 oxidation in the MDCOs, the variation of Hg^0 oxidation at different injection conditions was tested. As shown in Figure 5, the depletion of Hg^0 across the MDCOs (HCl injected from port 1) was monitored synchronously, and Hg^0 oxidation in the TCO mode was used for comparison (HCl injected from port 2). It can be seen that the Hg^0 concentration dropped quickly with the injection of HCl into the MDCOs, and it became stable within 100 min. At this moment, the efficiency of Hg^0 oxidation reached about 93% and the measured amount of escaped HCl was as low as 0.2 mg m^{-3}, while most of the injected HCl was retained in the MDCOs. Similarly, the concentration of escaped HCl was still lower than 0.5 and 2 mg m^{-3} even the duration of HCl injection into the MDCOs was 4 and 7 h, respectively. If HCl injection stopped after 4 h, then the conversion efficiency of Hg^0 can remain over 90% for about an additional 4 h (curve b in Figure 5B). The result indicates that the injection of HCl can be operated intermittently in practice (e.g., every 3−4 h), in which the utilization efficiency of HCl was higher and its escape to the simulated gas can be minimized.

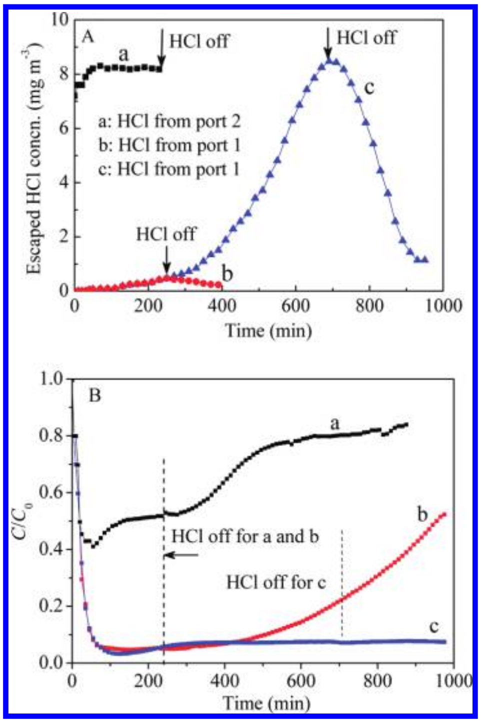

FIGURE 5. The HCl penetration curves (A) and depletion curves of Hg^0 (B) at 573 K: Initial HCl concentration inside the membrane was 200 mg m^{-3} (balanced with dry air). The injection flow rate of HCl was 1.0 L h^{-1} from port 1 for the MDCOs and port 2 for the TCO mode; The membrane was 50 mm in length with an ε of 8 wt.%; The total flow rate of the gas outside the membrane was 25.0 L h^{-1}; A(a) and B(a), 240 min of HCl injection in the TCO mode; A(b) and B(b), 240 min of HCl injection in the MDCOs; A(c) and B(c), 690 min of HCl injection in the MDCOs.

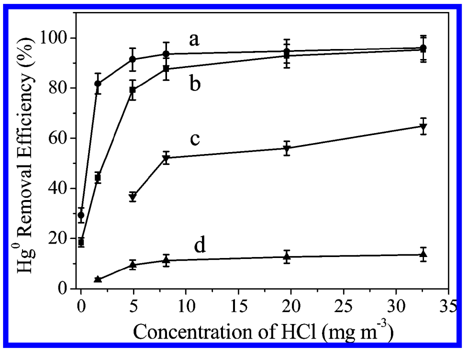

FIGURE 6. The effects of HCl concentration on the efficiency of Hg^0 removal in the MDCOs and TCO mode at 423 K and 573 K: The total flow rate of the gas outside the membrane was 25.0 L h^{-1} with air as the balance gas; The data were obtained at 200 min of HCl injection time. (a) 573 K, $\varepsilon = 8$ wt.%; (b) 423 K, $\varepsilon = 8$ wt.%; (c) 573 K, $\varepsilon = 8$ wt.% for the TCO mode; and (d) 573 K, $\varepsilon = 0$.

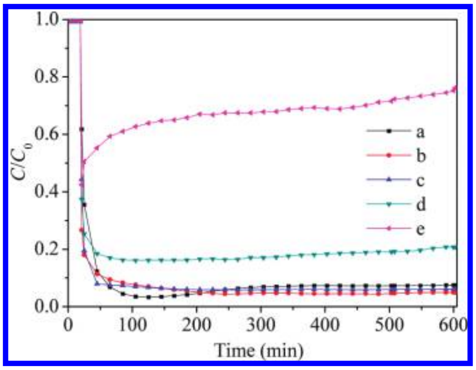

FIGURE 7. Effects of SO_2 on the efficiency of Hg^0 removal in the presence of 8.2 mg m^{-3} HCl at 573 K: Initial HCl concentration inside the membrane ($\varepsilon = 8\%$) was 200 mg m^{-3} (balanced with dry air). The injection flow rate of HCl was 1.0 L h^{-1} from port 1 for the MDCOs and port 2 for the TCO mode; The total flow rate of the gas outside the membrane was 25.0 L h^{-1}. (a) Without SO_2; (b) SO_2 concentration = 1500 mg m^{-3}; (c) SO_2 concentration = 2500 mg m^{-3}; (d) SO_2 concentration = 4000 mg m^{-3}; and (e) SO_2 concentration = 2500 mg m^{-3}, HCl injection at port 2 (TCO).

However, the oxidation efficiency of Hg^0 in the TCO mode was rather less than that in the MDCOs, and only about 50% of Hg^0 was oxidized with 8 mg m^{-3} of HCl. The oxidation efficiency of Hg^0 decreased quickly once HCl injection stopped. Almost all of the unreacted HCl in the TCO mode will directly escape with the simulated gas. Therefore, the amount of escaped HCl in the TCO mode was ten times more than that in the MDCOs with the intermittent injection of HCl.

In addition, the efficiencies of Hg^0 conversion as a function of HCl concentration were investigated and the results are illustrated in Figure 6. As expected, HCl displayed a significant effect on Hg^0 oxidation in the presence of MnO_x catalyst. The efficiencies of Hg^0 conversion went up with the increase of equivalent HCl concentration. When HCl concentration was about 1.6 mg m^{-3}, the efficiency of Hg^0 conversion at 573 K was about 82%, and it reached about 91% in the presence of 5.0 mg m^{-3} of HCl. Then, the efficiency of Hg^0 oxidation became flat with higher HCl concentration. However, it was just about 56.0% even with 19.6 mg m^{-3} of HCl in the TCO mode. The results clearly indicate that HCl in the MDCOs can be effectively utilized because of the favored gas−solid exposure and preactivation of HCl on the surface of the catalysts. It can be estimated that Hg^0 conversion in the MDCOs would demand less than 5% of the amount of HCl demanded in the TCO mode.

Meanwhile, it was found that there existed good agreement between the converted Hg^0 and the produced Hg^{2+} across the MDCOs in the presence of HCl when the reaction process became stable, with the balance of 96 (±8)% for the total mercury between in the inlet gas (Hg^0) and the outlet gas (Hg^{2+} and Hg^0) (Figure S7 and Table S1 in the SI).

The effect of the temperature on the efficiencies of Hg^0 oxidation in the MDCOs was also shown in Figure 6. The efficiency of Hg^0 oxidation at 423 K was just slightly lower than that at 573 K at various HCl concentrations, which was consistent with our previous work with the TCO mode (*11*), but the difference of the efficiency between the two temperatures was much smaller in the MDCOs. The results imply that Hg^0 oxidation in the MDCOs can occur more easily at lower temperature than that in the TCO mode because of the favorable exposure and activation condition of HCl and the catalysts.

Effects of SO_2 and NO in the MDCOs. Three concentrations of SO_2 were involved in the simulated flue gas. As shown in Figure 7, SO_2 displayed an insignificant effect on Hg^0 oxidation in the MDCOs even when its concentration in the gas was up to 2500 mg m^{-3}. However, SO_2 exerted more severe inhibition to Hg^0 oxidation in the TCO mode, and the efficiency of Hg^0 oxidation decreased from about 52% (without SO_2) to 36% with 2500 mg m^{-3} of SO_2. Therefore, Hg^0 oxidation in the MDCOs displayed a better resistance to SO_2 than in the TCO.

The SO_2 inhibition to Hg^0 oxidation has been mainly attributed to the competitive adsorption for catalyst active sites between HCl and SO_2 (*11*), and thus to interfere with Deacon reaction to produce active species (Cl_2 or Cl). However, there still lacks a direct evidence to address it. In order to have a better understanding on this aspect, SO_2 adsorption in the presence of HCl was further determined in the TCO and MDCOs, respectively (Figure S7 in the SI).

It was found that the amount of SO_2 adsorbed on the surface of catalysts decreased dramatically in the MDCOs compared with the TCO mode in the presence HCl. Therefore, it has been demonstrated that the adsorption of SO_2 can be notably minimized in the MDCOs, and HCl is preferentially adsorbed on the available active sites of the catalysts, which was helpful to increase the Hg^0 conversion and minimize the inhibition of SO_2.

In this work, the effects of NO on Hg^0 oxidation was investigated by varying its concentration from 100−300 mg m^{-3} with various concentration of SO_2 (2500 and 4000 mg m^{-3}). It was found that NO displayed a slightly promotional effect on Hg^0 oxidation in the MDCOs. Although it has ever been reported that NO showed obvious inhibition to Hg^0 oxidation by gas-phase reaction (*5, 14, 15*), much research has manifested that its effects are insignificant to the heterogeneous catalytic reaction (*16*). Moreover, some researchers have proposed that there might exist a weak synergistic effect between HCl and NO in the presence of metal catalysts (*10*), e.g., $NO_{(ad)}$ can combine with $[Cl]^*_{(ad)}$ to form unstable $NOCl^*_{(ad)}$, then HgCl is produced by the reaction of $NOCl^*_{(ad)}$ and $Hg_{(ad)}$. However, further research is still necessary to reveal such complicated facts.

Discussion on the Mechanism of Hg^0 Oxidation in the MDCOs. The fact that Hg^0 catalytic conversion in the MDCOs is more effective than in the TCO mode can be mainly attributed to the unique mass transfer way of HCl. As shown in Figure 1, given that the adsorbed HCl concentration on the catalyst surface is equal (i.e., $C_{sa} = C_{sb}$), the demanded HCl in the MDCOs might be by far less than that in the TCO mode (i.e., $[X]_b \ll [X]_a$). In addition, the amount of escaped HCl in the MDCOs is expected to be quite low at $C_{sa} = C_{sb}$, because there exist series of mass transfer resistance and concentration gradients during the escape process of HCl. Moreover, the HCl delivery mode in the MDCOs ensures its exposure to the catalyst preferentially, which might be helpful to minimize the competitive adsorption against SO_2 for the active sites. The aspects have been well supported by the foregoing results.

The XPS technology was also used to identify the chemical state of the adsorbed mercury and MnO_x on the catalysts (Figure S7 and S8 in the SI). Compared to the Mn 2p XPS spectrum database of NIST (*17*), MnO_x on the catalysts was determined to be present mainly in the states of Mn(IV) besides a little in Mn(III), which was consistent with the XRD results. It was found that the adsorbed mercury on the surface of catalysts was mainly in the form of HgO in the absence of HCl, but in the presence of HCl, it was mainly in bivalent form ($HgCl_2$) in the gas, which is readily volatile from the catalyst surface over 373 K.

The mechanism for the capture of Hg^0 with HCl by MnO_2/Al_2O_3 can be written as follows (*9*):

$$Hg_{(g)} + \text{surface} \rightarrow Hg_{(ad)} \tag{3}$$

$$HCl_{(g)} + \text{surface} \rightarrow HCl_{(ad)} \tag{4}$$

$$HCl_{(ad)} + \equiv Mn^{IV} \rightarrow [Cl]^*_{(ad)} + \equiv Mn^{III} + H^+ \tag{5}$$

$$Hg_{(ad)} + [Cl]^*_{(ad)} \rightarrow HgCl_{(ad)} \tag{6}$$

$$HgCl_{(ad)} + [Cl]^*_{(ad)} \rightarrow HgCl_{2(ad)} \tag{7}$$

$$O_{2(g)} + \text{surface} \rightarrow O_{2(ad)} \tag{8}$$

$$4 \equiv Mn^{III} + O_{2(ad)} \rightarrow 4 \equiv Mn^{IV} + 2 \equiv O \tag{9}$$

where $\equiv Mn^{IV}$, $\equiv Mn^{III}$, $\equiv O$, and $[Cl]^*_{(ad)}$are Mn^{4+}, Mn^{3+}, O^{2-} and reactive activated Cl on the surface of MnO_2/Al_2O_3, respectively. The overall reaction for Hg^0 oxidation can be expressed with eq 10.

$$2Hg_{(g)} + 4HCl_{(g)} + O_{2(g)} \xrightarrow{MnO_2} 2HgCl_{2(ad)} + 2H_2O_{(ad)} \tag{10}$$

Reactions 3, 4, and 8 are the collision of gas-phase mercury, gaseous HCl, and gaseous oxygen with the surface of the sorbents, respectively, resulting in physical adsorption. Reactions 5, 6, and 7 are the formations of reactive activated Cl ($[Cl]^*_{(ad)}$) and the reaction process of $Hg_{(ad)}$ and $[Cl]^*_{(ad)}$, respectively. Reaction (9) is the regeneration of Mn^{4+} cations by gaseous oxygen.

Recent studies have also indicated that atomic chlorine (reactive activated Cl, $[Cl]^*_{(ad)}$) was the primary chlorine-containing specie responsible for oxidizing Hg^0 via the reactions 6 and 7, and the contribution by gas phase reaction between Hg^0 and HCl or even Cl_2 was insignificant (*5, 18−20*). The previous studies with SCR also gave similar hints for Hg^0 conversion approaches (*4, 13*).

In addition, how to make good use of the MDCOs units in industrial applications needs an elaborated design. The proposed assembly shown in Figure S9 in the SI might be one of the options, in which every tubular MDCO unit can be directly installed on the duct (or the enlarged duct) of flue gas in rows with knocked-down mode. Therefore, it has been demonstrated that a higher Hg^0 conversion efficiency can be obtained with lower HCl consumption in the MDCOs compared with the TCO mode, and the inhibition of SO_2 was also less significant as well. The MDCOs appear to be promising modes for the conversion of elemental mercury from coal-fired flue gas with HCl, and it might be also an innovation in environmental catalysis.

Acknowledgments

This work was supported by the High-Tech R&D Program of China (863) under Grant No. 2007AA06Z340 and NSFC Project (21077073). Special thanks to Dr. Juan Wang, Jianfeng Li, and Jie Chen for their help in mercury sampling and analysis.

Supporting Information Available

FE-SEM images of the virgin ceramic, pore size distribution curve of catalysts, analysis of EDX spectrum, content of adsorbed chlorine on the catalyst surface, role of O_2, adsorption curves of SO_2, mass balance analysis of mercury, XPS analysis, and discussion on the potential assembly of the MDCOs in application. This information is available free of charge via the Internet at http://pubs.acs.org/.

Literature Cited

(1) Podak, B.; Brunetti, M.; Lewis, A.; Wilcox, J. Mercury binding on activated carbon. *Environ. Prog.* **2006**, *25* (4), 319–326.

(2) Galbreath, K. C.; Zygarlicke, C. J. Mercury transformations in coal combustion flue gas. *Fuel Process. Technol.* **2000**, *65*, 289–310.

(3) Chang, J. C. S.; Ghorishi, S. B. Simulation and evaluation of elemental mercury concentration increase in flue gas across a wet scrubber. *Environ. Sci. Technol.* **2003**, *37* (24), 5763–5766.

(4) He, S.; Zhou, J. S.; Zhu, Y. Q.; Luo, Z. Y.; Ni, M. J.; Cen, K. F. Mercury oxidation over a vanadia-based selective catalytic reduction catalyst. *Energy Fuel.* **2009**, *23* (1), 253–259.

(5) Norton, G. A.; Yang, H. Q.; Brown, R. C.; Laudal, D. L.; Dunham, G. E.; Erjavec, J. Heterogeneous oxidation of mercury in simulated post combustion conditions. *Fuel* **2003**, *82* (2), 107–116.

(6) Uddin, M. A.; Ozaki, M.; Sasaoka, E.; Wu, S. J. Temperature-programmed decomposition desorption of mercury species over activated carbon sorbents for mercury removal from coal-derived fuel gas. *Energy Fuel.* **2009**, *23*, 4710–4716.

(7) Wu, Z. B.; Jiang, B. Q.; Liu, Y. Effect of transition metals addition on the catalyst of manganese/titania for low-temperature selective catalytic reduction of nitric oxide with ammonia. *Appl. Catal., B* **2008**, *79* (4), 347–355.

(8) Cao, Y.; Gao, Z.; Zhu, J.; Wang, Q.; Huang, Y.; Chiu, C.; Parker, B.; Chu, P.; Pan, W. P. Impacts of halogen additions on mercury oxidation, in a slipstream selective catalyst reduction (SCR), reactor when burning sub-bituminous coal. *Environ. Sci. Technol.* **2008**, *42* (1), 256–261.

(9) Presto, A. A.; Granite, E. J. Noble metal catalysts for mercury oxidation in utility flue gas gold, palladium and platinum formulations. *Platinum Metals Rev.* **2008**, *52* (3), 144–154.

(10) Hrdlicka, J. A.; Seames, W. S.; Mann, M. D.; Muggli, D. S.; Horabik, C. A. Mercury oxidation in flue gas using gold and palladium catalysts on fabric filters. *Environ. Sci. Technol.* **2008**, *42* (17), 6677–6682.

(11) Qiao, S. H.; Chen, J.; Li, J. F.; Qu, Z.; Liu, P.; Yan, N. Q.; Jia, J. P. Adsorption and catalytic oxidation of gaseous elemental mercury in flue gas over MnO_x/Alumina. *Ind. Eng. Chem. Res.* **2009**, *48* (7), 3317–3322.

(12) Li, J. F.; Yan, N. Q.; Qu, Z.; Qiao, S. H.; Yang, S. J.; Guo, Y. F.; Liu, P.; Jia, J. P. Catalytic oxidation of elemental mercury over the modified catalyst Mn/alpha-Al_2O_3 at lower temperatures. *Environ. Sci. Technol.* **2010**, *44* (1), 426–431.

(13) Cao, Y.; Chen, B.; Wu, J.; Cui, H.; Smith, J.; Chen, C. K.; Chu, P.; Pan, W. P. Study of mercury oxidation by a selective catalytic reduction catalyst in a pilot-scale slipstream reactor at a utility boiler burning bituminous coal. *Energy Fuel.* **2007**, *21* (1), 145–156.

(14) Li, Y.; Murphy, P.; Wua, C. Y. Removal of elemental mercury from simulated coal-combustion flue gas using a SiO_2-TiO_2 nanocomposite. *Fuel Process. Technol.* **2008**, *89* (6), 567–573.

(15) Chi, Y.; Yan, N. Q.; Qu, Z.; Qiao, S. H.; Jia, J. P. The performance of iodine on the removal of elemental mercury from the simulated coal-fired flue gas. *J. Hazard. Mater.* **2009**, *166* (2−3), 776–781.

(16) Krishnakumar, B.; Helble, J. J. Understanding mercury transformations in coal-fired power plants: Evaluation of homogeneous Hg oxidation mechanisms. *Environ. Sci. Technol.* **2007**, *41* (22), 7870–7875.

(17) NIST XPS Database. http://srdata.nist.gov/xps/(accessed Aug. 2007).

(18) Zhao, Y. X.; Mann, M. D.; Pavlish, J. H.; Mibeck, B. A. F.; Dunham, G. E.; Olson, E. S. Application of gold catalyst for mercury oxidation by chlorine. *Environ. Sci. Technol.* **2006**, *40* (5), 1603–1608.

(19) Yan, N. Q.; Liu, S. H.; Chang, S. G.; Miller, C. Method for the study of gaseous oxidants for the oxidation of mercury gas. *Ind. Eng. Chem. Res.* **2005**, *44* (15), 5567–5574.

(20) Qiao, Y.; Xu, M. H. The oxidation kinetics of mercury in Hg/O/H/Cl system. *Dev. Chem. Eng. Miner. Process.* **2005**, *13* (3−4), 483–494.

ES1020586